

Quantum confinement of carriers in the type-I quantum wells structure

Xinxin Li(李欣欣), Zhen Deng(邓震), Yang Jiang(江洋), Chunhua Du(杜春花), Haiqiang Jia(贾海强), Wenxin Wang(王文新), and Hong Chen(陈弘)

Citation: Chin. Phys. B, 2024, 33 (**9**): 097301. DOI: 10.1088/1674-1056/ad5d99
Journal homepage: http://cpb.iphy.ac.cn; http://iopscience.iop.org/cpb

What follows is a list of articles you may be interested in

Reanalysis of energy band structure in the type-II quantum wells

Xinxin Li(李欣欣), Zhen Deng(邓震), Yang Jiang(江洋), Chunhua Du(杜春花), Haiqiang Jia(贾海强), Wenxin Wang(王文新), and Hong Chen(陈弘)
Chin. Phys. B, 2024, 33 (**6**): 067302. DOI: 10.1088/1674-1056/ad36bc

Design and investigation of doping-less gate-all-around TFET with Mg_2Si source material for low power and enhanced performance applications

Pranav Agarwal, Sankalp Rai, Rakshit Y. A, and Varun Mishra
Chin. Phys. B, 2023, 32 (**10**): 107310. DOI: 10.1088/1674-1056/acd5c0

Energy band and charge-carrier engineering in skutterudite thermoelectric materials

Zhiyuan Liu(刘志愿), Ting Yang(杨婷), Yonggui Wang(王永贵), Ailin Xia(夏爱林), and Lianbo Ma(马连波)
Chin. Phys. B, 2022, 31 (**10**): 107303. DOI: 10.1088/1674-1056/ac6ee8

Fabrication of sulfur-doped cove-edged graphene nanoribbons on Au(111)

Huan Yang(杨欢), Yixuan Gao(高艺璇), Wenhui Niu(牛雯慧), Xiao Chang(常霄), Li Huang(黄立), Junzhi Liu(刘俊治), Yiyong Mai(麦亦勇), Xinliang Feng(冯新亮), Shixuan Du(杜世萱), and Hong-Jun Gao(高鸿钧)
Chin. Phys. B, 2021, 30 (**7**): 077306. DOI: 10.1088/1674-1056/abfbd0

High-performance self-powered photodetector based on organic/inorganic hybrid van der Waals heterojunction of rubrene/silicon

Yancai Xu(徐彦彩), Rong Zhou(周荣), Qin Yin(尹钦), Jiao Li(李娇), Guoxiang Si(侣国翔), and Hongbin Zhang(张洪宾)
Chin. Phys. B, 2021, 30 (**7**): 077304. DOI: 10.1088/1674-1056/abf345

Quantum confinement of carriers in the type-I quantum wells structure

Xinxin Li(李欣欣)[1,2,†], Zhen Deng(邓震)[1,2,3,†], Yang Jiang(江洋)[1,2], Chunhua Du(杜春花)[1,2,3], Haiqiang Jia(贾海强)[1,2,4], Wenxin Wang(王文新)[1,2,4], and Hong Chen(陈弘)[1,2,3,4,‡]

[1] *Key Laboratory for Renewable Energy, Beijing Key Laboratory for New Energy Materials and Devices, Beijing National Laboratory for Condensed Matter Physics, Institute of Physics, Chinese Academy of Sciences, Beijing* 100190, *China*
[2] *Center of Materials and Optoelectronics Engineering, University of Chinese Academy of Sciences, Beijing* 100049, *China*
[3] *The Yangtze River Delta Physics Research Center, Liyang* 213000, *China*
[4] *Songshan Lake Materials Laboratory, Dongguan* 523808, *China*

(Received 15 June 2024; revised manuscript received 26 June 2024; accepted manuscript online 2 July 2024)

Quantum confinement is recognized to be an inherent property in low-dimensional structures. Traditionally, it is believed that the carriers trapped within the well cannot escape due to the discrete energy levels. However, our previous research has revealed efficient carrier escape in low-dimensional structures, contradicting this conventional understanding. In this study, we review the energy band structure of quantum wells along the growth direction considering it as a superposition of the bulk material dispersion and quantization energy dispersion resulting from the quantum confinement across the whole Brillouin zone. By accounting for all wave vectors, we obtain a certain distribution of carrier energy at each quantized energy level, giving rise to the energy subbands. These results enable carriers to escape from the well under the influence of an electric field. Additionally, we have compiled a comprehensive summary of various energy band scenarios in quantum well structures relevant to carrier transport. Such a new interpretation holds significant value in deepening our comprehension of low-dimensional energy bands, discovering new physical phenomena, and designing novel devices with superior performance.

Keywords: energy band, quantum confinement, type-I quantum wells, low-dimensional structures

PACS: 73.21.Fg, 73.20.At, 73.63.–b **DOI:** 10.1088/1674-1056/ad5d99

1. Introduction

Quantum confinement is considered to be an inherent property in low-dimensional material structures, which has attracted enormous attention in the fields of optoelectronics,[1,2] microelectronics,[3,4] and quantum physics.[5,6] Typically, the quantum confinement effect refers to the phenomenon where the behavior of particles is influenced by quantum mechanics. Such kinds of effects appear when the carriers are confined in a length scale comparable to or smaller than the de Broglie wavelength, resulting in discrete energy levels.[7] The unique electronic energy band structure because of the quantum confinement effect leads to many novel physical and optical properties,[8–10] which are utilized for devices with better performance. For example, quantum tunneling diodes with tunneling current as the main current component have been applied in low-power and high-speed circuits due to their efficient electronic transmission.[11–13] In addition, the study of quantum confinement effects has also promoted the establishment of band theory for low-dimensional materials, which reveals the essence of carriers' motion in the microscopic world with the quantum theory concept. Therefore, band analysis has become a powerful tool not only for understanding material properties but also for predicting the physical and chemical properties of the system to achieve better device performance.[14–17]

After years of in-depth research, we have experimentally observed the great carrier extraction efficiency (more than 85%) in InGaN multiple quantum wells (MQWs),[18–20] InGaAs MQWs,[21,22] and other low-dimensional materials systems[23,24] in PIN structures, as shown in Table 1. Such a high carrier extraction efficiency in low-dimensional systems is exciting, especially in the case of thick barrier ($>$ 10 nm) and high potential. Moreover, the carrier extraction efficiency can be further improved (over 90%) by applying reverse bias. These phenomena indicate that the efficient carrier extraction phenomenon in PIN structure does not originate from thermal excitation[25] or tunneling[26] as suggested in studies. The NIN structures with the same low-dimensional structure have also been studied in the same way, but high extraction efficiency did not occur as that in PIN structures because of the carrier blocking in the well.[27] However, in classical views, it is believed that the photo-generated carriers in the low-dimensional structures cannot escape from the potential well to form the photocurrent but can only relax to the bottom of the ground state and then recombine due to the discrete energy levels,[28] known as the quantum confinement of

†These authors contributed equally to this work.
‡Corresponding author. E-mail: hchen@iphy.ac.cn

© 2024 Chinese Physical Society and IOP Publishing Ltd

carriers. Obviously, the theory of discrete energy levels in low-dimensional QWs is no longer suitable for analyzing the anomalous photo-generated carriers' extraction in the QWs structure under the PN junction. Since the properties of the MQWs system are often understood through the band structures, it is necessary to go back to reanalyze the energy band structure in order to identify the essence of the phenomenon.

In this paper, the energy band structure of the type-I QWs along the growth direction is reanalyzed and considered as the superposition of the dispersion of bulk material and the dispersion of quantized energy from the quantum confinement within the whole Brillouin zone, rather than the discrete energy levels at a certain vector given in the traditional band theory. There is a certain energy distribution of the carrier's energy band in real space, making it possible for carriers to escape from the QW under the build-in electric field. Moreover, various cases for energy bands of the type-I QW structures have been summarized for carrier transportation, confirming the high possibility of carrier escape, which provides a good explanation for the efficient carrier extraction found in previous studies. This understanding of the energy bands can serve as a supplementary explanation to the traditional energy band theory of low-dimensional quantum confinement systems.

Table 1. The great carrier extraction efficiency in the low-dimensional PIN structures of our previous researches.

Structures	Active region	Well thickness (nm)	Well energy gap (E_g)	Barrier thickness (nm)	Barrier energy gap (E_g)	Extraction efficiency (%) (@0 V)	Ref.
Quantum wells	(InGaAs/GaAs) ×10	5	~ 1.2	20	1.43	87.3	[21]
	(InGaN/GaN) ×10	2.5	2.7	14	3.4	96.5	[19]
	(InGaN/GaN) ×10	2.5	2.7	12	3.4	95.15	[18]
Quantum dots	InAs/GaAs	diameter: 20 height: 6	0.41	50	1.43	88	[23]

2. Results and discussion

The main feature of the MQWs structure is that the barrier thickness is thicker so that the interaction between the QWs can be ignored, and the structure can be considered as a periodic repetition of a single QW.[28] Therefore, when analyzing the energy band structure of MQWs structure, we can simplify it as analyzing a single QW's energy band. Figure 1(a) gives the typical illustration of the single MQW structure with a growth direction along the z-axis, which is composed of alternating semiconductor thin layers with different bandgaps. When the thickness of one layer (blue) is comparable to the electron's de Broglie wavelength, the wave function that could originally propagate freely is confined by the yellow layer materials on both sides, resulting in the quantum confinement of carriers in the z direction. Here, the energy alignment of the well and barriers in the type-I single QW is shown in Fig. 1(b) for a schematic explanation. The energy gaps of the well and the barrier are E_{g1} and E_{g2}, while the blue and yellow areas correspond to energy distributions of the well and the barrier layers, respectively. For the equilibrium heterojunction, the chemical potential determines the energy arrangement of the well and barrier based on the phase equilibrium conditions,[29] resulting in discontinuities in the conduction and valence bands. To better understand the discontinuity of the energy, the energies of the well and barriers in Fig. 1(b) are displayed in the same $\boldsymbol{k}_z$ vector, as shown in Fig. 1(c). It is this discontinuity or the so-called band offset that plays a crucial role in confining electrons or holes in a QW structure and ultimately leads to quantum behavior.[30] The classical band theory only considers the quantum confinement effect at a certain $\boldsymbol{k}_z$ vector when dealing with quantum well electronic states, for example, the Γ point. Although thin, the quantum well (blue layer) usually has a thickness of nanometers or tens of nanometers, which means that there are at least tens or hundreds of atoms in the growth direction. When these atoms are close

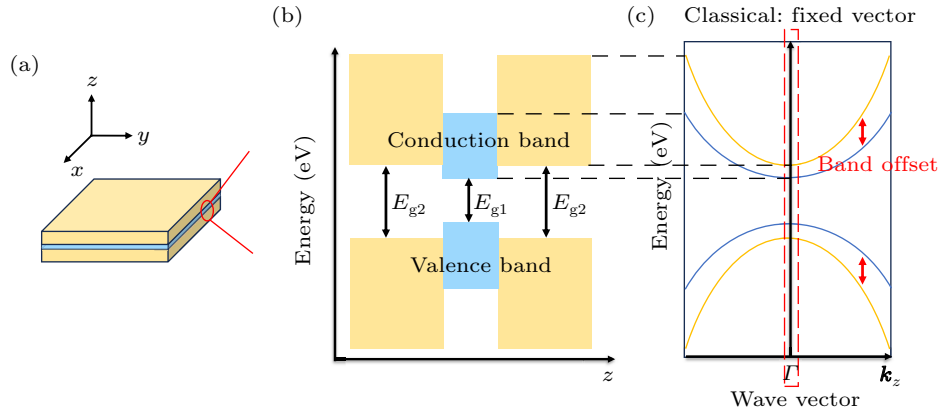


Fig. 1. (a) The typical illustration of the single QW structure. (b) The schematic diagram of the type-I energy alignment of the well and barriers in (a). (c) The schematic diagram of the bulk energy dispersions of the well and barrier in the same k-space.

to each other, they cause energy level splitting. This is overlooked in the classical band theory when dealing with electronic states in QWs, but it is crucial in our opinion as it may cause significant changes in key properties of low-dimensional structures. Thus, different from the discrete energy levels at a certain $\boldsymbol{k}_z$ vector given in the traditional band theory, the real energy dispersion of a type-I QW structure along the growth direction should be a combination of the dispersion of the material in the well and additional energy elevation caused by the quantum confinement effect within the whole Brillouin zone.

As analyzed above, the energy E_z along the z direction of the carriers in the well consists of two parts

$$E_z = E_z^{\mathrm{b}} + E_z^{\mathrm{s}}, \tag{1}$$

where E_z^{b} represents the energy resulting from the interaction of crystal cells while E_z^{s} is the quantized energy caused by quantum confinement.

The methods for the calculation of energy E_z^{b} in bulk materials include the tight binding approximation method (TBA),[31] the orthogonal plane-wave method (OPW), the $k\cdot p$ method,[32] the pseudopotential method,[33] etc. The main process is to solve the single electron Schrödinger equation in a periodic external field, which is not illustrated in detail here. As for the quantized energy E_z^{s} caused by the quantum confinement, the band offset is one of the key parameters determining energy level lifting. Assuming that the type-I QW is an ideal square potential well that the quantized energy E_z^{s} can be obtained by solving the Schrödinger equation in the one-dimensional potential well with finite depth. The potential value is the band offset obtained from the difference of E_z^{b} dispersions (see Fig. 1(c)). Thus, the Schrödinger equation for stationary states in the position basis in the well is given as[34]

$$\begin{aligned} &-\frac{\hbar^2}{2m^*_{(\boldsymbol{k}_z)}}\frac{\mathrm{d}^2}{\mathrm{d}z^2}\psi_{E_z^{\mathrm{s}}(\boldsymbol{k}_z)}(z) + V_{(\boldsymbol{k}_z)}(z)\,\psi_{E_z^{\mathrm{s}}(\boldsymbol{k}_z)}(z) \\ &= E^{\mathrm{s}}_{z\,(\boldsymbol{k}_z)}\psi_{E_z^{\mathrm{s}}(\boldsymbol{k}_z)}(z), \end{aligned} \tag{2}$$

where $m^*_{(\boldsymbol{k}_z)}$ is the effective mass of the carrier, z is the position, $\boldsymbol{k}_z$ is the wave vector, $\psi_{E_z^{\mathrm{s}}(\boldsymbol{k}_z)}(z)$ is the wave function of the particle corresponding to the quantized energy $E^{\mathrm{s}}_{z\,(\boldsymbol{k}_z)}$, and $V_{(\boldsymbol{k}_z)}(z)$ is the well potential generated by the band offset.

The Schrödinger equation presented here aims to solve the quantized energy levels at all vectors. In this scenario, the effective mass $m^*_{(\boldsymbol{k}_z)}$ varies with different $\boldsymbol{k}_z$ vectors,[35] as does the well-potential $V_{(\boldsymbol{k}_z)}$ due to the varying band offsets,[30]

$$m^*_{(\boldsymbol{k}_z)} = \begin{cases} m^*_{\mathrm{w}(\boldsymbol{k}_z)} = \dfrac{\hbar^2}{\left(\dfrac{\mathrm{d}^2 E_z^{\mathrm{b-w}}{}_{(\boldsymbol{k}_z)}}{\mathrm{d}\boldsymbol{k}_z^2}\right)}, & |z| < \frac{a}{2}, \\ m^*_{\mathrm{b}(\boldsymbol{k}_z)} = \dfrac{\hbar^2}{\left(\dfrac{\mathrm{d}^2 E_z^{\mathrm{b-b}}{}_{(\boldsymbol{k}_z)}}{\mathrm{d}\boldsymbol{k}_z^2}\right)}, & \frac{l}{2} > |z| \geq \frac{a}{2}, \end{cases} \tag{3}$$

$$V_{(\boldsymbol{k}_z)}(z) = \begin{cases} 0, & |z| < \frac{a}{2}, \\ V_{(\boldsymbol{k}_z)} = E_z^{\mathrm{b-b}}{}_{(\boldsymbol{k}_z)} - E_z^{\mathrm{b-w}}{}_{(\boldsymbol{k}_z)}, & \frac{l}{2} > |z| \geq \frac{a}{2}, \end{cases} \tag{4}$$

where $m^*_{\mathrm{w}(\boldsymbol{k}_z)}$ is the effective mass of the carrier in the well, $m^*_{\mathrm{b}(\boldsymbol{k}_z)}$ is the effective mass of the carrier in the barrier, $E_z^{\mathrm{b-w}}$ is the energy dispersion in the well, $E_z^{\mathrm{b-b}}{}_{(\boldsymbol{k}_z)}$ is the energy dispersion in the barrier, a is the well thickness, and l is the period thickness of the QW.

The method for solving the above Eq. (2) of different $\boldsymbol{k}_z$ vectors consists of writing the general forms of the wave functions inside and outside the well, and then matching the values and slopes at the boundary to solve for the unknown constants. Assuming that $0 \leq E^{\mathrm{s}}_{z\,(\boldsymbol{k}_z)} < V_{(\boldsymbol{k}_z)}$, the general solutions of Eq. (2) are[36]

$$\psi_{E_z^{\mathrm{s}}(\boldsymbol{k}_z)} = A\sin\alpha z + B\cos\alpha z, \quad |z| < \frac{a}{2}, \tag{5}$$

$$\psi_{E_z^{\mathrm{s}}(\boldsymbol{k}_z)} = C\mathrm{e}^{-\beta z} + D\mathrm{e}^{\beta z}, \quad \frac{l}{2} > |z| \geq \frac{a}{2}, \tag{6}$$

where

$$\alpha = \frac{\sqrt{2E^{\mathrm{s}}_{z\,(\boldsymbol{k}_z)} m^*_{\mathrm{w}(\boldsymbol{k}_z)}}}{\hbar}, \quad \beta = \frac{\sqrt{2(V_{(\boldsymbol{k}_z)} - E^{\mathrm{s}}_{z\,(\boldsymbol{k}_z)}) m^*_{\mathrm{b}(\boldsymbol{k}_z)}}}{\hbar},$$

A, B, C, and D are constants to be determined.

Application of the boundary conditions (continuity and continuity of derivatives) at $|z| = a/2$ and $|z| = l/2$ gives the transcendental equations about β and α, and the energy spectrum of $E^{\mathrm{s}}_{z\,(\boldsymbol{k}_z)}$ at different $\boldsymbol{k}_z$ vectors will be determined by the values of β and α.

To better understand the real energy E_z in the type-I QW structure as mentioned above, in particular to clarify the mechanisms of how the carriers effectively run out of the well, a schematic diagram is drawn in Fig. 2(a). The green line represents the energy dispersion of the bulk material (E_z^{b}) along the z-direction, while the red line represents the dispersion of the quantized energy level due to quantum confinement (taking the ground state E^{s}_{z0} as an example). When two types of energies are superimposed, the whole energy dispersion of E_{z0} becomes the blue line in Fig. 2(a), which exhibits a certain range of energy in the whole Brillouin zone. In this case, there is a high probability for the carriers at the $\boldsymbol{k}_z$ vector (the red point) transporting to higher energy along the dispersion curve (see the yellow arrow in Fig. 2(a)), as long as the additional required energy is provided. When an electric field exists, the carriers in the well can obtain the required energy and momentum for transportation through the continuous interaction with the lattice. While in classical band theory, the increase in carriers' energy under an electric field is unlikely to compensate for the large gap between the quantized energy levels at one time, leading to the failure of transportation. The dispersion E_z in Fig. 2(a) is transferred into the real space for demonstration purposes, which only focuses on the distribution range of energy, as shown in Fig. 2(b). As we can see, the blue

lines in the well in Fig. 2(b) are the quantized energy level E_{z0} of electrons at Γ point, while the blue shaded area represents the energy distribution of the E_{z0} in real space appearing as a subband rising from the blue energy level. The whole energy bands structure in the real space for carriers in the type-I QW structure is given in Fig. 2(c), where the blue shaded area and the yellow shaded area represent the energy bands of electrons and holes in real space, respectively, and the green and red shaded areas are the energy bands in the barrier. One thing for sure is that for both electrons and holes in the well, there is a subband arising from each quantized energy (blue lines for electrons, green lines for light holes, and red lines for heavy holes) when considering all the vectors in the whole Brillouin zone. As long as the subband states in the well can extend above the barrier energy, there is a high possibility for carriers to escape from the well with the help of the electric field.

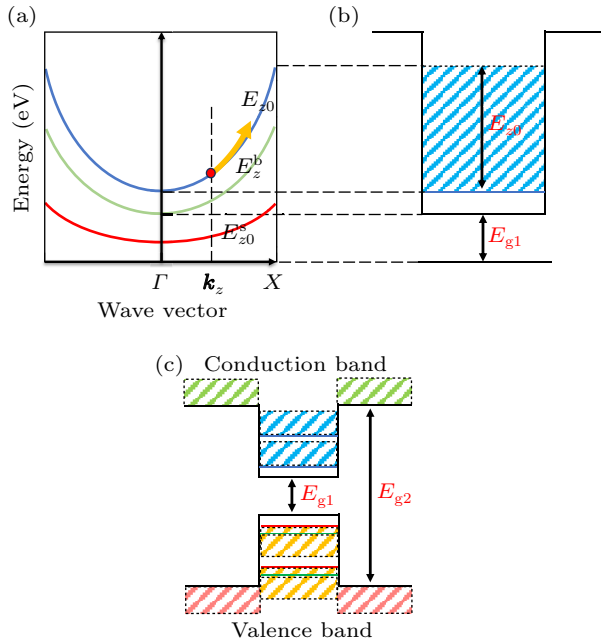


Fig. 2. (a) The schematic diagram of energy dispersion E_z consists of the energy dispersion (E_z^b) of the bulk material and dispersion of the quantum energy level E_z^s due to quantum confinement with all the vectors. (b) The energy subband structure in the real space for electrons from the energy dispersion E_{z0} in (a). (c) The whole energy band structure in the real space for carriers in the type-I QW structure.

Table 2. The 16 permutations of energy bands for carriers in the type-I QW structure. Here Y and N represent the conditions of the transportation described in Fig. 3(a) are met and not, respectively, while the red and black letters correspond to the electrons and holes, respectively. For example, the YNYN means that for both electrons and holes, the condition of transportations-1 is met while the condition of transportations-2 is not.

	NN	NY	YN	YY
NN	NNNN	NNNY	NNYN	NNYY
NY	NYNN	NYNY	NYYN	NYYY
YN	YNNN	YNNY	YNYN	YNYY
YY	YYNN	YYNY	YYYN	YYYY

According to the energy bands for carriers in the QW structure shown in Fig. 2(b), we attempt to analyze the possible scenarios of the energy bands. The transportation of the carriers (electrons or holes) in the type-I QW is shown in Fig. 3(a), assuming that there are two subbands in the well. Transportations-1 (Trans-1): there is no gap between the subbands in the well, allowing carriers to transport from one to another under an electric field. Transportations-2 (Trans-2): there is no gap between the higher subband in the well and the band in the barrier, allowing carriers to transport out of the well under the electric field. The energy bands for carriers in the type-I QWs structure in Fig. 3(a) can be summarized into 16 permutations according to these transportations, as shown in Table 2. The letters Y and N represent the conditions of the transportation described in Fig. 3(a) are met and not, respectively, while the red and black letters correspond to the electrons and holes, respectively. For example, the YNYN means that for both electrons and holes, the condition of Trans-1 is met while the condition of Trans-2 is not. For both electrons and holes, the conditions for carriers escaping from the well are very strict. Typically, only when both Trans-1 and Trans-2 are simultaneously fulfilled, can the carriers (electrons or holes) finally escape from the well. In addition, because of the existence of the Coulomb effect, both electrons and holes must fulfill the escape conditions at the same time to ensure the realization of carriers' escape. Considering these limitations, the 16 mentioned permutations can be categorized into two cases: the carriers can escape (YYYY) or cannot (the others). Furthermore, the energy bands for carriers in the type-I QW structure based on these 16 permutations are displayed with more intuitive diagrams in Figs. 3(b)–3(f). As shown in Figs. 3(b)–3(d) (NN__, NY__, and YN__), there are energy gaps in the well due to the small widths of the electrons' subbands that Trans-1 and Trans-2 for electrons cannot be allowed simultaneously, resulting in the confinement of electrons. In this situation, carriers cannot escape from the well due to Coulomb interaction whatever the energy bands of the holes are. Similarly, when the electrons can escape but the holes are still confined in the well, effective carrier escape still cannot occur, as exhibited in Fig. 3(e). Only when both electrons and holes can be extracted simultaneously, can the effective escape of carriers be achieved, as displayed in Fig. 3(f). Unfortunately, even if the conditions of carrier escape are harsh, the probability of the YYYY permutation is very high since the conduction and valance bands are usually very wide, which is why we obtained great carrier escape efficiencies in our experimental measurements as Table 1 shows. Certainly, the escape of carriers in the well is also related to the external conditions of well thickness and strength of the built-in electric field since they jointly determine the drift time of the carriers in the well, which will affect the competition between escape and relaxation-recombination processes during transportation. If the drift time is greater than the relaxation-recombination time, the carriers in the well will mainly be consumed in the

form of recombination and cannot escape from the well. Our discussion provides a direction to find out the quantum confined condition for carriers in the well from the internal perspective of the band structure.

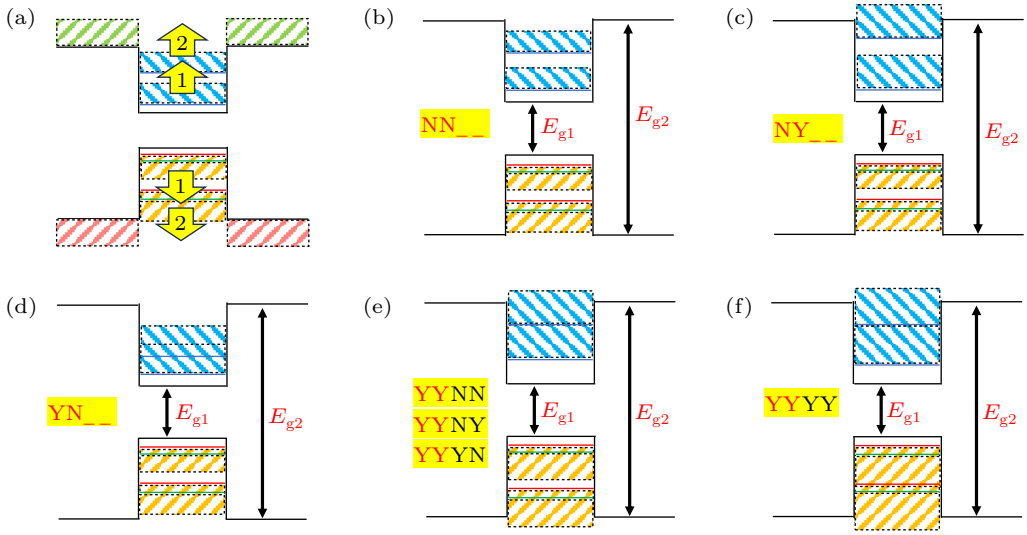


Fig. 3. (a) Two transportations of carriers (electrons or holes) in the well. Transportations-1: carriers transport from one subband to the other. Transportations-2: carriers transport from the higher subband in the well to the band in the barrier. (b)–(d) The energy bands for carriers in the type-I QW structure corresponding to the permutations described in the first row (NN__), second row (NY__), and third row (YN__) of Table 2, respectively. (e) The energy bands for carriers in the type-I QW structure with permutations of YYNN, YYNY, YYYN described in Table 2. (f) The energy bands for carriers in the type-I QW structure with the permutation of YYYY described in Table 2.

The band structure is an important semiconductor parameter, shaping numerous physical and chemical properties of low dimensional structures represented by quantum wells, such as electrical, optical, physicochemical, and other characteristics. Consequently, any alterations in the band structure inevitably result in modifications to the internal properties of the structures. Such changes could prompt a renewed comprehension of quantum effects and necessitate reinterpretation of experimental results. Furthermore, with this new comprehension of band structure in low-dimensional structure, it is expected to achieve special devices with novel characteristics under the strong built-in electric field of the P–N junction and promote technological innovation in semiconductor optoelectronic conversion application fields. For instance, the high probability of carrier escape within QWs enables the creation of photodetectors using inter-band transitions, which is considered to be difficult to succeed in traditional band theories.

3. Conclusion

In conclusion, after reanalyzing the energy bands of the type-I MQWs structure, we believe that in the confinement direction, the real energy E_z of the carriers consists of two parts, one is the dispersion E_z^{b} of the bulk material and the other is the dispersion E_z^{s} of quantized energy caused by quantum confinement within the whole Brillouin zone, rather than the discrete energy levels given at a certain vector in the traditional band theory. The energy distribution of the carrier's energy leads to the band formation, making it possible for carriers to escape from the well under an electric field. Based on this, multiple possibilities for energy bands in the type-I QW structure have been summarized for carrier transportation. Such supplementary explanation to the traditional band theory would significantly assist the discovery of new physics phenomena and the development of novel semiconductor devices.

Acknowledgments

Project supported by the National Natural Science Foundation of China (Grant Nos. 61991441 and 62004218), the Strategic Priority Research Program of Chinese Academy of Sciences (Grant No. XDB01000000), and Youth Innovation Promotion Association of Chinese Academy of Sciences (Grant No. 2021005).

References

[1] Köhler R, Tredicucci A, Beltram F, Beere HE, Linfield E H, Davies A G, Ritchie D A, Iotti R C and Rossi F 2002 *Nature* **417** 156
[2] Wang H X, Fu Z L, Shao D X, Zhang Z Z, Wang C, Tan Z Y, Guo X G and Cao J C 2018 *Appl. Phys. Lett.* **113** 171107
[3] Yang M J, Wang F C, Yang C H, Bennett B R and Do T Q 1996 *Appl. Phys. Lett.* **69** 85
[4] Ferry D K, Weinbub J, Nedjalkov M and Selberherr S 2022 *Semicond. Sci. Technol.* **37** 043001
[5] Fu H L, Yan J J, Wu Y J, Zhang R X, Sun J, Shan P J, Wang P J, Zhu Z Y, Pfeiffer L N, West K W, Liu H W, Xie X C and Lin X 2019 *Nat. Commun.* **10** 4351
[6] Liu C X, Qi X L, Dai X, Fang Z and Zhang S C 2008 *Phys. Rev. Lett.* **101** 146802
[7] Gaponenko S V and Demir H V 2018 *Applied Nanophotonics* (Cambridge: Cambridge University Press) pp. 52–91
[8] Brum J A and Bastard G 1986 *Phys. Rev. B* **33** 1420
[9] Barbagiovanni E G, Lockwood D J, Simpson P J and Goncharova L V 2014 *Appl. Phys. Rev.* **1** 011302

[10] Kalt H and Klingshirn C F 2019 *Semiconductor Optics 1: Linear Optical Properties of Semiconductors* 5th Edn. (Chan: Springer International Publishing) pp. 251–271
[11] Day D J, Chung Y, Webb C, Eckstein J N, Xu J M and Sweeny M 1990 *Appl. Phys. Lett.* **57** 1260
[12] Althib H 2021 *Results Phys.* **22** 103943
[13] Encomendero J, Yan R S, Verma A, Islam S M, Protasenko V, Rouvimov S, Fay P, Jena D and Xing H G 2018 *Appl. Phys. Lett.* **112** 103101
[14] Gu Y, Zhang Y G, Ma Y J, Zhou L, Chen X Y, Xi S P and Du B 2015 *Appl. Phys. Lett.* **106** 121102
[15] Yahyazadeh R 2021 *Opt. Quantum Electron.* **53** 571
[16] Xue J, Zhao Y J, Oh S H, Herrington W F, Speck J S, DenBaars S P, Nakamura S and Ram R J 2015 *Appl. Phys. Lett.* **107** 121109
[17] Chen B L 2017 *IEEE Trans. Electron Devices* **64** 1606
[18] Wu H Y, Ma Z G, Jiang Y, Wang L, Yang H J, Li Y F, Zuo P, Jia H Q, Wang W X, Zhou J M, Liu W M and Chen H 2016 *Chin. Phys. B* **25** 117803
[19] Yang H J, Ma Z G, Jiang Y, Wu H Y, Zuo P, Zhao B, Jia H Q and Chen H 2017 *Sci. Rep.* **7** 43357
[20] Li Y F, Jiang Y, Die J H, Wang C W, Yan S, Wu H Y, Ma Z G, Wang L, Jia H Q Wang W X and Chen H 2018 *Chin. Phys. B* **27** 097104
[21] Sun Q L, Wang L, Jiang Y, Ma Z G, Wang W Q, Sun L, Wang W X, Jia H Q, Zhou J M and Chen H 2016 *Chin. Phys. Lett.* **33** 106801
[22] Liu J, Wang L, Sun L, Wang W Q, Wu H Y, Jiang Y, Ma Z G, Wang W X, Jia H Q and Chen H 2018 *Acta Phys. Sin.* **67** 128101 (in Chinese)
[23] Wang W Q, Wang L, Jiang Y, Ma Z G, Sun L, Liu J, Sun Q L, Zhao B, Wang W X, Liu W M, Jia H Q and Chen H 2016 *Chin. Phys. B* **25** 097307
[24] Li X Z, Sun L, Lu J L, Liu J, Yue C, Xie L L, Wang W X, Chen H, Jia H Q and Wang L 2020 *Chin. Phys. B* **29** 038504
[25] Botha J R and Leitch A W R T 1994 *Phys. Rev. B* **50** 18147
[26] Emiliani V, Bonanni B, Frova A, Capizzi M, Martelli F and Stone S S 1995 *J. Appl. Phys.* **77** 5712
[27] Tang X S, Li X X, Yue C, Wang L, Deng Z, Jia H Q, Wang W X, Ji A C, Jiang Y and Chen H 2020 *Appl. Phys. Express* **13** 071009
[28] Grundmann M 2010 *The Physics of Semiconductors* 2nd Edn. (Heidelberg: Springer-Verlag) pp. 369–374
[29] Milnes A G and Feucht D L 1976 *Heterojunctions and Metal Semiconductor Junctions* (New York: Academic Press) pp. 1–33
[30] Nag B R 2000 *Physics of Quantum Well Devices* (Dordrecht: Kluwer Academic Publishers) pp. 22–34
[31] Chadi D J and Cohen M L 1975 *Phys. Status Solidi B* **68** 405
[32] Hermann C and Weisbuch C 1977 *Phys. Rev. B* **15** 823
[33] Schwerdtfeger P 2011 *ChemPhysChem* **12** 3143
[34] Schrödinger E 1926 *Ann. Phys. (Berlin)* **384** 489
[35] Kittel C 1956 *Introduction to Solid State Physics* 2nd Edn. (New York: John Wiley & Sons) p. 289
[36] Schiff L I 1968 *Quantum Mechanics* 3 Ed. (New York: McGraw-Hill Book Company) Vol. 2 pp. 19–44